CHAPTER 3

Computation of 2D and 3D High-order Discrete Orthogonal Moments

José S. Rivera-Lopez, César Camacho-Bello, and Lucia Gutiérrez-Lazcano

This chapter is about eliminating numerical instability and the error of high-order orthogonal moments by reducing terms in existing recurrence relations and the Gram-Smith orthonormalization process. Besides, the simplification of the terms of the recurrence relations with respect to n of the most used kernels is analyzed, such as Tchebycheff polynomials, Hahn polynomials, Krawtchouk polynomials, Charlier polynomials, and Meixner polynomials. Also, to guarantee the effectiveness of the proposed method, reconstructions of both 3D objects and high-resolution images are presented. The results presented in this chapter will help you utilize moments for processing, recognition, and analysis on 8K Full HD images and 3D objects with large dimensions.

José S. Rivera-Lopez, César Camacho-Bello, Lucia Gutiérrez-Lazcano
Universidad Politécnica de Tulancingo
Tulancingo, Mexico
e-mail: josesaul9@hotmail.com, cesar.camacho@upt.edu.mx, lucia.gutierrez@upt.edu.mx

Editor: G.A. Papakostas, *Recent Progress in Image Moments and Moment Invariants*
DOI: 10.15579/gcsr.vol7.ch3, GCSR Vol. 7, pp. 53-74, 2021

3.1 Introduction

In recent years there has been an increasing interest in the processing and recognition of 3D objects and color images with high resolutions. In general, the kernel of the moments is defined by the hypergeometric function, which uses operations that require a higher degree of computational complexity. Also, the computation of high-order orthogonal moments is limited by numerical instability, making it difficult to calculate the moments, seriously affecting the quality of the image reconstruction. Mukundan R. [11] uses the recurrence relation in the x-direction to reduce numerical instability caused by the propagation of numerical errors based on the recurrence relation in the n-direction. Moreover, Zhu, H. et al. [18] proposed a general form for obtaining discrete orthogonal moments, which shows that the recurrence relations in x-direction have better performance; unfortunately, they present numerical instability for orders greater than 1000. In order to solve this problem, the recurrence relation in x and n direction are used sequentially depending on the properties of each family of discrete moments, as described for the Tchebichef moments [2], Charlier moments [1], and Krawtchouk moments [10]. However, a problem encountered when computing high order polynomials are the propagation of numerical errors when using any recursive formula. A pivotal remedy to address this problem is the effective use of the recurrence relation to achieving a certain degree of stability. Recently, Camacho-Bello and Rivera-Lopez [4] proposed to remove the carry error to compute higher-order Tchebichef polynomials using the Gram-Schmidt process and the recurrence relation with respect to n. On the other hand, there are other works with a similar approach, such as Hahn moments [15, 7], Charlier moments [9, 8], and Meixner moments [6].

This chapter presents the reduction of the number of operations for the recurrence relation with respect to n of the different kernels of the discrete orthogonal moments to reduce the numerical instability. This work analyzes the reduction of terms in the recurrence relations with respect to n of the most used kernels, such as Tchebichef polynomials, Hahn polynomials, Krawtchouk polynomials, Charlier polynomials, and Meixner polynomials. Unlike the most current methods for calculating high-order moments with the Gram-Smith orthonormalization process. Likewise, reconstructions of both 3D objects and images with high resolution are presented to guarantee the effectiveness of the proposed method; the Dragon from the Stanford repository [5] with dimensions of $400 \times 1000 \times 500$ voxels, and a collection of 12 images from the TEST IMAGES database [3] to form an image of 9600×9600 pixels. The results presented in this chapter will help utilize the moments for processing, recognition, and analysis in 8K Full HD images and 3D objects with large dimensions. The presented analysis help to have a better representation of some of the studied families of discrete orthogonal moments.

3.2 Discrete Orthogonal Moments

Given an orthogonal basis in a finite-dimensional vector space, any element of said vector space can be represented as a linear combination of the base. On the other hand, the moments of a random sample are the expected values of specific functions that form a collection of descriptive measures that characterize a sample. Therefore, from a discrete orthogonal base, different families of moments can be defined that provide linearly independent characteristics of a sample. Moments can be calculated as one-dimensional, two-dimensional, and three-dimensional, as shown below.

The set of one-dimensional orthogonal discrete moments of order n is defined as follows:

$$\phi_n = \sum_{x=0}^{N-1} \widetilde{p}_n\left(x;N\right) f\left(x\right) \tag{3.1}$$

where $n = 0, 1, 2, ..., N$ and $f(x)$ is a one-dimensional signal of size N.

The set of two-dimensional orthogonal discrete moments of orders (n, m) is defined as follows :

$$\phi_{n.m} = \sum_{x=0}^{N-1} \sum_{y=0}^{M-1} \widetilde{p}_n\left(x;N\right) \widetilde{p}_m\left(y;M\right) f\left(x,y\right) \tag{3.2}$$

where $n = 0, 1, 2, \ldots, N-1$, $m = 0, 1, 2, \ldots, M-1$, and $f\left(x,y\right)$ it is a digital image with size $N \times M$.

The computation of three-dimensional discrete orthogonal moments of order (n, m, k) is defined as:

$$\phi_{n,m,k} = \sum_{x=0}^{N-1} \sum_{y=0}^{M-1} \sum_{z=0}^{K-1} \widetilde{p}_n(x;N)\widetilde{p}_m(y;M)\widetilde{p}_k(z;K)f(x,y,z) \tag{3.3}$$

where $n = 0, 1, 2, \ldots N-1$, $m = 0, 1, 2, \ldots, M-1$, $k = 0, 1, 2, \ldots, K-1$, and $f\left(x,y,y\right)$ is a 3D object of size $N \times M \times K$.

It is essential to preserve the orthogonality condition of the orthogonal base of the moments to guarantee that the moment characteristics of a signal, image, or object are linearly independent and do not contain redundant information. The next section shows a strategy for the kernel computation of moments that helps us preserve orthogonality for any order.

3.3 Kernel Computation of Discrete Moments

The calculation of the high-order orthogonal polynomial base causes a numerical instability that makes it difficult to calculate the moments, seriously affecting the orthogonality and the quality of the reconstruction. To solve this problem, Camacho-Bello and Rivera-Lopez [4] use the Gram-Schmidt approximation to guarantee the orthogonality of the polynomials calculated through the recurrence relation with respect to n. The Gram-Schmidt orthonormalization process is an algorithm that constructs a set of orthonormal vectors, starting from a collection of linearly independent vectors of a vector space, up to another set of orthonormal vectors that generates the same subspace, developed by the mathematicians Jorgen Gram and Erhardt Schmidt [13]. By using the Gram-Schmidt orthogonalization process during the calculation of the nucleus of the moments, it allows us to solve the problem of numerical instability when using higher-order moments since the orthogonality property is not affected. On the other hand, the kernel of the discrete moments is calculated using recurrence relationships, which leads to the propagation and accumulation of numerical errors. In general, the computation of classical orthogonal polynomials uses generalized recurrence relations with respect to the order n. Zhu, H. et al. [18] propose a generalization of the calculation of polynomials with respect to the order n of the classic discrete orthogonal polynomials, which are defined as follows,

$$A * \widetilde{p}_n(x) = B * D\widetilde{p}_{n-1}(x) + C * E\widetilde{p}_{n-2}(x) \tag{3.4}$$

where the coefficients A, B, C, D, E are considered as independent variables. One strategy to decrease the spread of the accumulated error is to simplify the number of operations of the terms of the recurrence relations. It is easy to algebraically reduce the parameters of the Eq.(3.4), as follows,

$$\widetilde{p}_n(x) = \frac{B * D * \widetilde{p}_1(x) + C * E * \widetilde{p}_0(x)}{A}, \tag{3.5}$$

in this way, it is possible to carry out the operations of the terms $\frac{B*D}{A}$, and $\frac{C*E}{A}$ to simplify the recurrence relation of the discrete orthogonal polynomials. The reduction is defined as follows,

$$A_n * \widetilde{p}_n(x) = B_n * \widetilde{p}_1(x) - A_{n-1} * \widetilde{t}_0(x). \tag{3.6}$$

In the same way that the recurrence relation of three terms requires the polynomials of zero-order $\widetilde{p}_0(x)$ and first-order $\widetilde{p}_1(x)$ to start the calculation. Taking into account the problem of calculating discrete orthogonal polynomials through a recurrence relation such as Eq. (3.4).The following subsections show a proposal to perform the calculation of the Tchebichef, Krawtchouk, Hahn, Meixner, and Charlier polynomials by simplifying operations such as the gamma function and factorials, in the same way reducing operations algebraically and modifying the relationship of recurrence of Eq. (3.4).

3.3.1 Tchebychef Polynomials

Thebichef polynomials were first used as a moments kernel by Mukundan et al. [12]. In the same way, the reduction of terms is performed for the polynomials Tcebychef $\widetilde{t}_n(x; N))$, using their values of A, B, C, D, E proposed by Zhu, H. et al [18],

$$\begin{aligned} A &= \frac{n}{2(2n-1)}, \\ B &= x - \frac{N-1}{2}, \\ C &= -\frac{(n-1)[N^2-(n-1)^2]}{2(2n-1)}, \\ D &= \sqrt{\frac{2n+1}{(N^2-n^2)(2n-1)}}, \\ E &= \sqrt{\frac{2n+1}{(N^2-n^2)[N^2-(n-1)^2](2n-3)}}. \end{aligned} \tag{3.7}$$

The first calculation simplification of $\frac{B*D}{A}$ is given by,

$$\begin{aligned} \frac{B*D}{A} &= \frac{\left(x-\frac{N-1}{2}\right)\sqrt{\frac{2n+1}{(N^2-n^2)(2n-1)}}}{\frac{n}{(2n-1)}}, \\ &= \frac{(2x-N+1)\sqrt{(2n+1)(2n-1)}}{n\sqrt{(N^2-n^2)}}. \end{aligned} \tag{3.8}$$

The second simplification $\frac{C*E}{A}$ can see as,

$$\begin{aligned} \frac{C*E}{A} = \frac{\left(-\frac{(n-1)[N^2-(n-1)^2]}{2(2n-1)}\right)\sqrt{\frac{2n+1}{(N^2-n^2)[N^2-(n-1)^2](2n-3)}}}{\frac{n}{(2n-1)}}, \\ = -\frac{(n-1)\sqrt{(N^2-(n-1)^2)(2n+1)}}{n\sqrt{(N^2-n^2)(2n-3)}}. \end{aligned} \tag{3.9}$$

By substituting Eqs. (3.8) and (3.9) in the recurrence relation of Eq. (3.4) is obtained,

$$\begin{aligned} \tilde{t}_n(x) = \frac{(2x-N+1)\sqrt{(2n+1)(2n-1)}}{n\sqrt{(N^2-n^2)}}\tilde{t}_1(x) - \\ \frac{(n-1)\sqrt{(N^2-(n-1)^2)(2n+1)}}{n\sqrt{(N^2-n^2)(2n-3)}}\tilde{t}_0(x), \end{aligned} \tag{3.10}$$

and can be rewritten as follows,

$$\begin{aligned} n\sqrt{(N^2-n^2)}\tilde{t}_n(x) = (2x-N+1)\sqrt{(2n+1)(2n-1)}\tilde{t}_1(x) - \\ \frac{(n-1)\sqrt{(N^2-(n-1)^2)(2n+1)}}{\sqrt{2n-3}}\tilde{t}_0(x). \end{aligned} \tag{3.11}$$

Algorithm 3.1 Tchebychef polynomials orthonormalization with the Gram-Schmidt process.

$B_n \leftarrow (2x - N + 1)\sqrt{(2n+1)(2n-1)}\ \forall x = 0, 1, 2, \ldots, N-1$
$A_{n-1} \leftarrow (n-1)\sqrt{[N^2 - (n-1)^2]}$
$t_0\left(x; N\right) \leftarrow \frac{1}{\sqrt{N}}$
$t_1\left(x; N\right) \leftarrow (2x - N + 1)\sqrt{\frac{3}{(N(N^2-1))}}$
for $n = 2$ to $N - 1$ **do**
  $A_n \leftarrow n\sqrt{N^2 - n^2}$
  $t_{n+1}\left(x; N\right) \leftarrow \frac{B_n}{A_n} t_n\left(x; N\right) - \frac{A_{n-1}}{A_n} t_{n-1}\left(x; N\right)$
  $A_{n-1} \leftarrow A_n$
  $T\left(x; N\right) \leftarrow t_{n+1}\left(x; N\right)$
  for $k = 0$ to n **do**
    $t_{n+1}\left(x; N\right) \leftarrow t_{n+1}\left(x; N\right) - \left[\sum_{x=0}^{N-1} T\left(x; N\right) t_k\left(x; N\right)\right] \times t_k\left(x; N\right)$
  end for
  $h \leftarrow \sqrt{\sum_{x=0}^{N-1} \left[t_{n+1}\left(x; N\right)\right]^2}$
  $t_{n+1}\left(x; N\right) \leftarrow \frac{t_{n+1}(x;N)}{h}$
end for

Using the recurrence relation of Eq. (3.6) we obtain the values of A_n and B_n for the calculation of the Thebichef polynomials from Eq. (3.11)

$$A_n = n\sqrt{(N^2 - n^2)}, \tag{3.12}$$

$$B_n = (2x - N + 1)\sqrt{(2n+1)(2n-1)}, \tag{3.13}$$

Finally, the initial values $\tilde{t}_0(x; N)$ and $\tilde{t}_1(x; N)$ are given by,

$$\begin{aligned} \tilde{t}_0(x; N) &= \sqrt{\frac{1}{N}}, \\ \tilde{t}_1(x; N) &= (2x - N + 1)\sqrt{\frac{3}{(N(N^2-1))}} \end{aligned} \tag{3.14}$$

The calculation of the Tchebichef polynomials with the proposed recurrence relation and the orthogonalization process is shown in Algorithm 3.1. In Fig. 3.1a shows the graphical representation for high-order Tchebichef polynomial.

3.3.2 Krawtchouk Polynomials

Krawtchouk polynomials were introduced by Mikhail Krawtchouk and applied in the image analysis by Yap et al. [16]. Krawtchouk moments are suitable for extracting local characteristics from any region of interest of an image by adjusting the parameter p of the binomial distribution associated with the Krawtchouk polynomials. Similarly, it is possible to carry out the same procedure for the reduction of terms of the discrete orthogonal polynomials. Returning to the $A-E$ values proposed by Zhu, H. et al. [18] for the Krawtchouk polynomials $\widetilde{k}_n(x;p,N)$,

$$\begin{aligned} A &= n, \\ B &= x-n+1-p(N-2n+2), \\ C &= -p(1-p)(N-n+2), \\ D &= \sqrt{\frac{n}{p(1-p)(N-n+1)}}, \\ E &= \sqrt{\frac{n(n-1)}{(p(1-p))^2(N-n+2)(N-n+1)}}. \end{aligned} \tag{3.15}$$

Performing the simplification of $\frac{B*D}{A}$ is given by

$$\begin{aligned} \frac{B*D}{A} &= \frac{(x-n+1-p(N-2n+2))\sqrt{\frac{n}{p(1-p)(N-n+1)}}}{n}, \\ &= \frac{x-n+1-p(N-2n+2)}{\sqrt{np(1-p)(N-n+1)}}, \end{aligned} \tag{3.16}$$

while that for,

$$\begin{aligned} \frac{C*E}{A} &= \frac{(-p(1-p)(N-n+2))\sqrt{\frac{n(n-1)}{(p(1-p))^2(N-n+2)(N-n+1)}}}{n}, \\ &= -\sqrt{\frac{(N-n+2)(n-1)}{n(N-n+1)}}, \end{aligned} \tag{3.17}$$

By substituting Eqs. (3.16) and (3.17) in the recurrence relation of Eq. (3.4). The reduced recurrence relation of the Krawtchouk polynomials is given by,

$$\begin{aligned} \sqrt{n(N-n+1)}\widetilde{k}_n(x) &= \frac{x-n+1-p(N-2n+2)}{\sqrt{p(1-p)}}\widetilde{k}_1(x) - \\ &\quad \sqrt{(N-n+2)(n-1)}\widetilde{k}_0(x), \end{aligned} \tag{3.18}$$

as was done in Eq. (3.11), using the recurrence relation of Eq. (3.6) we obtain the values of A_n and B_n for the calculation of the Krawtchouk polynomials from Eq. (3.18)

$$A_n = \sqrt{n}, \tag{3.19}$$

Algorithm 3.2 Krawtchouk polynomials orthonormalization with the Gram-Schmidt process.

$A_{n-1} \leftarrow \sqrt{N}$
$k_1(x;N) \leftarrow \sqrt{\frac{N!p^x(1-p)^{N-x}}{x!(N-x)!}}$
$k_2(x;N) \leftarrow (-p(N-x)+x(1-p)) * \sqrt{\frac{(N-1)!p^{x-1}(1-p)^{N-x-1}}{x!(N-x)!}}$
for $n=2$ to $N-1$ **do**
  $A_n \leftarrow \sqrt{n(N-n+1)}$
  $B_n \leftarrow \frac{x-n+1-p(N-2n+2)}{\sqrt{p(1-p)}}\ \forall x=0,1,2,\ldots,N-1$
  $k_{n+1}(x;N) \leftarrow \frac{B_n}{A_n}k_n(x;N) - \frac{A_{n-1}}{A_n}k_{n-1}(x;N)$
  $A_{n-1} \leftarrow A_n$
  $K(x;N) \leftarrow k_{n+1}(x;N)$
  for $i=0$ to n **do**
    $k_{n+1}(x;N) \leftarrow k_{n+1}(x;N) - \left[\sum_{x=0}^{N-1} K(x;N)\,k_i(x;N)\right] \times t_i(x;N)$
  end for
  $h \leftarrow \sqrt{\sum_{x=0}^{N-1}\left[k_{n+1}(x;N)\right]^2}$
  $k_{n+1}(x;N) \leftarrow \frac{k_{n+1}(x;N)}{h}$
end for

$$B_n = \frac{x-n+1-p(N-2n+2)}{\sqrt{p(1-p)}}, \tag{3.20}$$

The initial values for $\widetilde{k}_1(x)$ and $\widetilde{k}_0(x)$ are given by,

$$\begin{aligned} \widetilde{k}_0(x;p,N) &= \sqrt{\frac{N!p^x(1-p)^{N-x}}{x!(N-x)!}}, \\ \widetilde{k}_1(x;p,N) &= (-p(N-x)+x(1-p)) * \sqrt{\frac{(N-1)!p^{x-1}(1-p)^{N-x-1}}{x!(N-x)!}}. \end{aligned} \tag{3.21}$$

The calculation of the polynomials with the proposed recurrence relation and the orthogonalization process are shown in Algorithm 3.2. Fig. 3.1b shows the graphical representation for high-order Krawtchouk polynomials.

3.3.3 Hahn Polynomials

Hahn polynomials were defined by Wolfgang Hahn and used in the image analysis by Zhou et al. [17]. This set of polynomials is associated with the negative hypergeometric distribution and has two adjustable parameters a and b, which control the shape of the polynomials. Similarly, the reduction of terms is carried out for the Hahn polynomials $\tilde{h}_n^{(a,b)}(x;N)$, using the values of $A-E$ proposed by Zhu, H. et al. [18] defined as follows,

$$\begin{aligned} A &= \frac{n}{(a+b+2n-1)} * \frac{(a+b+n)}{(a+b+2n)}, \\ B &= x - \tfrac{a-b+2N-2}{4} - \tfrac{(b^2-a^2)(a+b+2N)}{4(a+b+2n-2)(a+b+2n)} \ , \\ C &= -\tfrac{(a+n-1)(b+n-1)}{(a+b+2n-2)} * \tfrac{(a+b+N+n-1)(N-n+1)}{(a+b+2n-1)} \ , \\ D &= \sqrt{\tfrac{n(a+b+n)(a+b+2n+1)}{(N-n)(a+b+2n-1)(a+n)(b+n)(a+b+n+N)}} \ , \\ E &= \sqrt{\tfrac{n(n-1)(a+b+n)}{(a+n)(a+n-1)(b+n)(b+n-1)(N-n+1)(N-n)}} \\ & \quad * \sqrt{\tfrac{(a+b+n-1)(a+b+2n+1)}{(a+b+2n-3)(a+b+n+N)(a+b+n+N-1)}} \ . \end{aligned} \tag{3.22}$$

Performing the simplification of $\frac{B*D}{A}$ we have,

$$\begin{aligned} \frac{B*D}{A} &= \left(x - \frac{a-b+2n-1}{4} - \frac{(b^2-a^2)(a+b+2N)}{4(a+b+2n-2)(a+b+2n)}\right) * \\ & \sqrt{\frac{n(a+b+n)(a+b+2n+1)}{(N-n)(a+n)(b+n)(a+b+2n-1)(a+b+n+N)}} * \\ & \left(\frac{(a+b+2n-1)(a+b+2n)}{n(a+b+n)}\right) \\ &= \frac{(a+b+2n)\sqrt{(a+b+2n-1)(a+b+n+N)}}{\sqrt{n(a+b+n)(N-n)(a+n)(b+n)(a+b+n+N)}} * \\ & \left(x - \frac{a+b+2n-2}{4} - \frac{(b^2-a^2)(a+b+2N)}{4(a+b+2n-2)}\right), \end{aligned} \tag{3.23}$$

while that for,

$$\frac{C*E}{A} = \left(-\frac{(a+n-1)(b+n-1)(a+b+N+n-1)(N-n+1)}{(a+b+2n-2)(a+b+2n-1)}\right)* \tag{3.24}$$
$$\sqrt{\frac{n(n-1)(a+b+n)}{n(n-1)(a+n-1)(b+n)(b+n-1)(N-n-1)(N-n)}}*$$
$$\sqrt{\frac{(a+b+n-1)(a+b+2n+1)}{(a+b+2n-3)(a+b+n+N)(a+b+n+N-1)}}*$$
$$\left(\frac{(a+b+2n-1)(a+b+2n)}{n(a+b+n)}\right)$$

$$= -\frac{(a+b+2n)\sqrt{(n-1)(a+b+n-1)(a+n-1)}}{(a+b+2n-2)\sqrt{n(a+b+n)(a+n)}}*$$
$$\frac{\sqrt{(b+n-1)(N-n+1)(a+b+N+n-1)(a+b+2n+1)}}{\sqrt{(b+n)(N-n)(a+b+N+n)(a+b+2n-3)}},$$

Again substituting Eqs. (3.23) and (3.24) in the recurrence relation of Eq. (3.4) and rewriting the equation,

$$\frac{\sqrt{n(a+b+n)(a+n)(b+n)(N-n)(a+b+N)}}{a+b+2n}\tilde{h}_n^{(a,b)}(x) \tag{3.25}$$

$$= \frac{a-b+2n-2}{4} + \frac{(b^2-a^2)(a+b+2N)}{4(a+b+2n-2)}\tilde{h}_1^{(a,b)}(x) -$$
$$\frac{\sqrt{(n-1)(a+b+n-1)(a+n-1)}}{(a+b+2n-1)}*$$
$$\frac{\sqrt{(b+n-1)(N-n+1)(a+b+N+n-1)(a+b+2n+1)}}{\sqrt{(a+b+2n-3)}}\tilde{h}_0^{(a,b)}(x).$$

The values of A_n and B_n for the calculation of Hahn's polynomials from Eq. (3.25) are given by,

$$A_n = \frac{\sqrt{n(a+b+n)(a+n)(b+n)(N-n)(a+b+N)}}{a+b+2n}, \tag{3.26}$$

$$B_n = \frac{a-b+2n-2}{4} + \frac{(b^2-a^2)(a+b+2N)}{4(a+b+2n-2)}, \tag{3.27}$$

The initial values for $\tilde{h}_0^{(a,b)}(x;N)$, and $\tilde{h}_1^{(a,b)}(x;N)$ are given by

Algorithm 3.3 Hahn polynomials orthonormalization with the Gram-Schmidt process.

$A_{n-1} \leftarrow \frac{\sqrt{(a+b+1)(a+1)(b+1)(N-1)(a+b+N)}}{a+b+2}$

$h_1(x;N) \leftarrow \sqrt{\frac{(a+1)_b(a+b+1)}{(N-a)_{b+1}}}$

$h_2(x;N) \leftarrow (a+b+2)\,x-(b+1)(N-1)\sqrt{\frac{a+b+3}{(a+1)(b+1)(N-1)(N+a+b+1)}}$

for $n=2$ to $N-1$ **do**

  $A_n \leftarrow \frac{\sqrt{n(a+b+n)(a+n)(b+n)(N-n)(a+b+N)}}{a+b+2n}$

  $B_n \leftarrow \frac{a-b+2n-2}{4}+\frac{(b^2-a^2)(a+b+2N)}{4(a+b+2n-2)}\ \forall x=0,1,2,\ldots,N-1$

  $h_{n+1}(x;N) \leftarrow \frac{B_n}{A_n}h_n(x;N)-\frac{A_{n-1}}{A_n}h_{n-1}(x;N)$

  $A_{n-1} \leftarrow A_n$

  $H(x;N) \leftarrow h_{n+1}(x;N)$

  for $k=0$ to n **do**

    $h_{n+1}(x;N) \leftarrow h_{n+1}(x;N)-\left[\sum_{x=0}^{N-1} H(x;N)\,h_k(x;N)\right]\times h_k(x;N)$

  end for

  $l \leftarrow \sqrt{\sum_{x=0}^{N-1}\left[h_{n+1}(x;N)\right]^2}$

  $h_{n+1}(x;N) \leftarrow \frac{h_{n+1}(x;N)}{l}$

end for

$$\begin{aligned} \overset{\sim(a,b)}{h_0}(x;N) &= \sqrt{\frac{w(x)}{d_0^2}}, \\ \overset{\sim(a,b)}{h_1}(x;N) &= ((a+b+2)x-(b+1)(N-1))\sqrt{\frac{w(x)}{d_0^2}}, \end{aligned} \tag{3.28}$$

The calculation of the Hahn polynomials with the proposed recurrence relation and the orthogonalization process are shown in Algorithm 3.3. Fig. 3.1c shows the graphical representation for high-order Hahn polynomial.

3.3.4 Meixner Polynomials

The set of Meixner polynomials proposed by Josef Meixner and applied in the analysis of grayscale images by Zhu et al. [19]. In the same way, the reduction of terms is carried out for the Meixner polynomials $\overset{\sim}{\varpi}_n^{(\beta,\mu)}(x)$. Returning to the values of $A-E$ proposed by Zhu, H. et al. [18],

$$\begin{aligned} A &= \frac{\mu}{\mu-1}, \\ B &= \frac{x - x\mu - n + 1 - \mu n + \mu - \beta\mu}{1-\mu}, \\ C &= \frac{(n-1)(n-2+\beta)}{1-\mu}, \\ D &= \sqrt{\frac{\mu}{n(\beta+n-1)}}, \\ E &= \sqrt{\frac{\mu^2}{n(n-1)(\beta+n-2)(\beta+n-1)}}. \end{aligned} \tag{3.29}$$

Performing the simplification of $\frac{B*D}{A}$, which is given by,

$$\begin{aligned} \frac{B*D}{A} &= \frac{\frac{x-x\mu-n+1-\mu n+\mu-\beta\mu}{1-\mu}\sqrt{\frac{\mu}{n(\beta+n-1)}}}{\frac{\mu}{\mu-1}}, \\ &= -\frac{(x-n+1+\mu(-x-n+1-\beta))\sqrt{\mu}}{\mu\sqrt{n(\beta+n-1)}}, \end{aligned} \tag{3.30}$$

while that for,

$$\begin{aligned} \frac{C*E}{A} &= \frac{\frac{(n-1)(n-2+\beta)}{1-\mu}\sqrt{\frac{\mu^2}{n(n-1)(\beta+n-2)(\beta+n-1)}}}{\frac{\mu}{\mu-1}}, \\ &= -\sqrt{\frac{(n-1)(n-2+\beta)}{n(\beta+n-1)}}. \end{aligned} \tag{3.31}$$

Substituting the Eqs. (3.30) and (3.31) in the recurrence relation of Eq. (3.4) and rewriting the equation is obtained,

$$\begin{aligned} \sqrt{n(\beta+n-1)}\tilde{\varpi}_n^{(\beta,\mu)}(x) = \frac{(x-n+1+\mu(-x-n+1-\beta))\sqrt{\mu}}{\mu\sqrt{n(\beta+n-1)}}\tilde{\varpi}_1^{(\beta,\mu)}(x) \\ -\sqrt{\frac{(n-1)(n-2+\beta)}{n(\beta+n-1)}}\tilde{\varpi}_0^{(\beta,\mu)}(x). \end{aligned} \tag{3.32}$$

The values of A_n and B_n for the computation of the Meixner polynomials of Eq. (3.32) are given as,

$$A_n = \sqrt{n(\beta+n-1)}, \tag{3.33}$$

Algorithm 3.4 Meixner polynomials orthonormalization with the Gram-Schmidt process.

$A_{n-1} \leftarrow \sqrt{\beta}$
$\varpi_1(x;N) \leftarrow \sqrt{\frac{\mu^x(\beta+x-1)!}{x!(\beta-1)!}(1-\mu)^\beta}$
$\varpi_2(x;N) \leftarrow (\beta + x - \frac{x}{\mu}) * \sqrt{\frac{\mu^x(\beta+x-1)!}{x!(\beta-1)!}\frac{\mu(1-\mu)^\beta}{\beta}}$
for $n = 2$ to $N-1$ **do**
  $A_n \leftarrow \sqrt{n(\beta+n-1)}$
  $B_n \leftarrow \frac{(x-n+1+\mu(-x-n+1-\beta))\sqrt{\mu}}{\mu}$ $\forall x = 0, 1, 2, \ldots, N-1$
  $\varpi_{n+1}(x;N) \leftarrow \frac{B_n}{A_n}\varpi_n(x;N) - \frac{A_{n-1}}{A_n}\varpi_{n-1}(x;N)$
  $A_{n-1} \leftarrow A_n$
  $\Omega(x;N) \leftarrow \varpi_{n+1}(x;N)$
  for $k = 0$ to n **do**
    $\varpi_{n+1}(x;N) \leftarrow \varpi_{n+1}(x;N) - \left[\sum_{x=0}^{N-1}\Omega(x;N)\varpi_k(x;N)\right] \times \varpi_k(x;N)$
  end for
  $h \leftarrow \sqrt{\sum_{x=0}^{N-1}\left[\varpi_{n+1}(x;N)\right]^2}$
  $\varpi_{n+1}(x;N) \leftarrow \frac{\varpi_{n+1}(x;N)}{h}$
end for

$$B_n = \frac{(x-n+1+\mu(-x-n+1-\beta))\sqrt{\mu}}{\mu}. \tag{3.34}$$

Finally, the initial values $\tilde{\varpi}_0^{(\beta,\mu)}(x)$ and $\tilde{\varpi}_1^{(\beta,\mu)}(x)$ are defined as,

$$\begin{aligned} \tilde{\varpi}_0^{(\beta,\mu)}(x) &= \sqrt{\frac{w(x)}{d_0^2}} = \sqrt{\frac{\mu^x(\beta+x-1)!}{x!(\beta-1)!}(1-\mu)^\beta}\ , \\ \tilde{\varpi}_1^{(\beta,\mu)}(x) &= (\beta+x-\frac{x}{\mu})\sqrt{\frac{w(x)}{d_1^2}} = (\beta+x-\frac{x}{\mu}) * \\ &\quad \sqrt{\frac{\mu^x(\beta+x-1)!}{x!(\beta-1)!}\frac{\mu(1-\mu)^\beta}{\beta}}\ . \end{aligned} \tag{3.35}$$

The calculation of the Meixner polynomials with the proposed recurrence relation and the orthogonalization process are shown in Algorithm 3.4. Fig. 3.1d shows the graphical representation for a high order Meixner polynomials.

3.3.5 Charlier Polynomials

The Charlier polynomials are a set of infinite discrete orthogonal polynomials defined by Carl Charlier and introduced in the image analysis by k. W. See et al. [14]. These polynomials are associated with the Poisson distribution and have adjustable parameters a_1 that control the shape of the polynomials. In the same way, the reduction of terms for the Charlier polynomials is carried out, using the values of $A-E$ proposed by Zhu, H. et al. [18],

$$\begin{aligned} A &= -a_1, \\ B &= x-n+1-a_1, \\ C &= n-1, \\ D &= \sqrt{\frac{a_1}{n}}, \\ E &= \sqrt{\frac{a_1^2}{n(n-1)}}. \end{aligned} \tag{3.36}$$

Performing the simplification of $\frac{B*D}{A}$ is given by

$$\begin{aligned} \frac{B*D}{A} &= \frac{(x-n+1-a_1)\sqrt{\frac{a_1}{n}}}{-a_1}, \\ &= -\frac{(x-n+1-a_1)\sqrt{a_1}}{a_1\sqrt{n}}, \end{aligned} \tag{3.37}$$

and $\frac{C*E}{A}$ is given by

$$\begin{aligned} \frac{C*E}{A} &= \frac{(n-1)\sqrt{\frac{a_1^2}{n(n-1)}}}{-a_1}, \\ &= -\frac{\sqrt{n-1}}{\sqrt{n}}. \end{aligned} \tag{3.38}$$

Substituting the Eqs. (3.37), and (3.38) in the recurrence relation of Eq. (3.4) rewriting the equation,

$$\sqrt{n}\tilde{C}_n^{a_1}(x) = -\frac{(x-n+1-a_1)\sqrt{a_1}}{a_1\sqrt{n}}\tilde{C}_1^{a_1}(x) - \frac{\sqrt{n-1}}{\sqrt{n}}\tilde{C}_0^{a_1}(x). \tag{3.39}$$

The values of A_n and B_n for the calculation of Charlier polynomials from Eq. (3.39) are given as,

$$A_n = \sqrt{n}, \tag{3.40}$$

$$B_n = -\frac{(x-n+1-a_1)\sqrt{a_1}}{a_1}, \tag{3.41}$$

Finally, the initial values $\tilde{C}_0^{a_1}(x)$ and $\tilde{C}_1^{a_1}(x)$ are defined by,

Algorithm 3.5 Charlier polynomials orthonormalization with the Gram-Schmidt process.

$A_{n-1} \leftarrow 1$
$c_1(x;N) \leftarrow \sqrt{\frac{e^{-a_1} a_1^x}{x!}}$
$c_2(x;N) \leftarrow \frac{a_1 - x}{a_1} \sqrt{\frac{e^{-a_1} a_1^{x+1}}{x!}}$
for $n = 2$ to $N-1$ **do**
  $A_n \leftarrow \sqrt{n}$
  $B_n \leftarrow -\frac{(x-n+1)\sqrt{a_1}}{a_1} \; \forall x = 0, 1, 2, \ldots, N-1$
  $c_{n+1}(x;N) \leftarrow \frac{B_n}{A_n} c_n(x;N) - \frac{A_{n-1}}{A_n} c_{n-1}(x;N)$
  $A_{n-1} \leftarrow A_n$
  $C(x;N) \leftarrow c_{n+1}(x;N)$
  for $k = 0$ to n **do**
    $c_{n+1}(x;N) \leftarrow c_{n+1}(x;N) - \left[\sum_{x=0}^{N-1} C(x;N)\, c_k(x;N)\right] \times c_k(x;N)$
  end for
  $h \leftarrow \sqrt{\sum_{x=0}^{N-1} \left[c_{n+1}(x;N)\right]^2}$
  $c_{n+1}(x;N) \leftarrow \frac{c_{n+1}(x;N)}{h}$
end for

$$\begin{aligned}\widetilde{C}_0^{a_1}(x) &= \sqrt{\frac{w(x)}{d_0^2}} = \sqrt{\frac{e^{-a_1} a_1^x}{x!}}\,, \\ \widetilde{C}_1^{a_1}(x) &= \frac{a_1 - x}{a_1}\sqrt{\frac{w(x)}{d_1^2}} = \frac{a_1 - x}{a_1}\sqrt{\frac{e^{-a_1} a_1^{x+1}}{x!}},\end{aligned} \tag{3.42}$$

The calculation of the Charlier polynomials with the proposed recurrence relation and the orthogonalization process are shown in Algorithm 3.5. Fig. 3.1e shows the graphical representation for high-order Charlier polynomials.

The source code of the proposed algorithms can be downloaded from the link.[1]

3.4 Large-size Images and Objects Reconstruction

Reconstruction is an inherent property of orthogonal moments, and they can characterize an image with a small set of moments. Furthermore, they can be reconstructed from a sufficiently large number of moments by the inverse transform. The reconstructed discrete distribution of the image is given by

$$\widetilde{f}(x,y) = \sum_{n=0}^{N-1} \sum_{m=0}^{M-1} \widetilde{p}_n(x;N)\, \widetilde{p}_m(y;M)\, \phi_{n,m} \tag{3.43}$$

1 https://github.com/JSaulRivera/Computation-of-2D-and-3D-high-order-discrete-orthogonal-moments.git

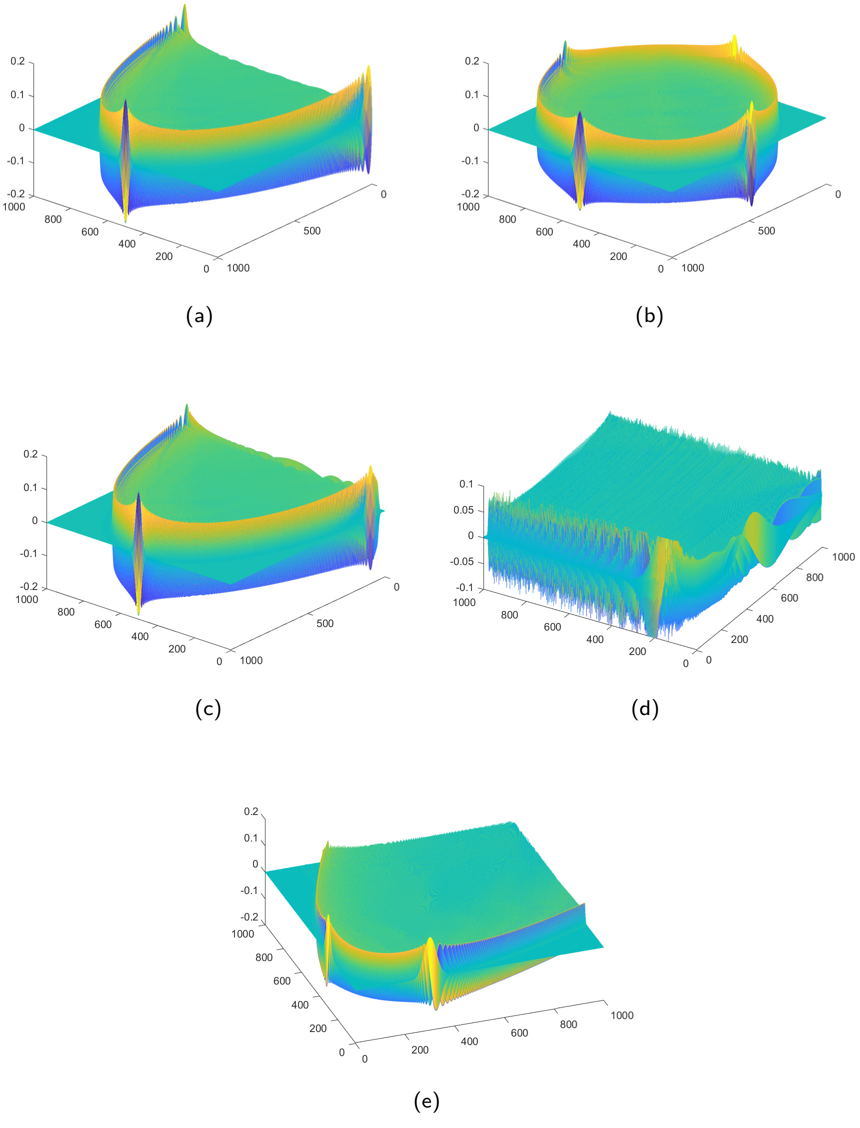

Figure 3.1: Graph of different discrete orthogonal polynomials with $n = 1, 2, 3, \ldots, 1000$. a) Tchebycheff, b) Krawtchouk ($p = 0.5$), c) Hahn ($a = 10, b = 10$), d) Meixner ($\mu = 0.9, \beta = 50$), and e) Charlier ($a_1 = 500$).

where $\widetilde{f}(x,y)$ is a reconstructed version of $f(x,y)$. On the other hand, a three-dimensional object $\widetilde{f}(x,y,z)$, can be reconstructed using the inverse transform of the computation of 3D moments as follows,

$$\widetilde{f}(x,y,z)=\sum_{n=0}^{N-1}\sum_{m=0}^{M-1}\sum_{k=0}^{K-1}\widetilde{p}_n(x;N)\widetilde{p}_m(y;M)\widetilde{p}_k(z;K)\Phi_{n,m,k} \tag{3.44}$$

where $\widetilde{f}(x,y,z)$, is the reconstruction obtained from $f(x,y,z)$. Algorithms 3.1 - 3.5 are used to guarantee the orthogonality of the kernel of the high order moments, which help to eliminate the accumulation of numerical error during the calculation of the high order polynomials; This helps to improve rebuilding performance. To demonstrate the effectiveness of the reduction of terms of the recurrence relations with respect to the order n and of the process of orthogonalization of Gram-Schmidt of the different families of classical orthogonal moments, the reconstruction of a composite FullHD image was carried out by a collection of 12 images from the TEST IMAGES database to form an image of 9600×9600 pixels [3] and the Dragon 3D from the Stanford repository [5] with dimensions of $400 \times 1000 \times 500$ voxels. Reconstruction results are shown in Figs. 3.2 and 3.3 using different families of moments and orders.

One way to evaluate the efficiency of the moment calculation is by means of the normalized image reconstruction error (NIRE) and it is defined as the normalized squared error between the input image $f(x,y)$ and the reconstructed image $\widetilde{f}(x,y)$ expressed as:

$$NIRE_{xy}=\frac{\sum_{x=0}^{N-1}\sum_{y=0}^{M-1}[f(x,y)-\widetilde{f}(x,y)]^2}{\sum_{x=0}^{N-1}\sum_{y=0}^{M-1}f^2(x,y)}. \tag{3.45}$$

Similarly, the normalized image reconstruction error for a 3D object is defined as,

$$NIRE_{xyz}=\frac{\sum_{x=0}^{N-1}\sum_{y=0}^{M-1}\sum_{z=0}^{K-1}\left[f(x,y,z)-\widetilde{f}(x,y,z)\right]^2}{\sum_{x=0}^{N-1}\sum_{y=0}^{M-1}\sum_{z=0}^{K-1}f^2(x,y,z)} \tag{3.46}$$

In Figs. 3.4 and 3.5 shows the graph of the error results obtained from the reconstruction of the 2D image and 3D object used for each one of the families of discreet moments.

The results of Figs. 3.2 and 3.3 show that when the order of reconstruction is equal to the size of the image, the Reconstruction error is equal to zero; this ensures that high-order discrete orthogonal polynomials satisfy the orthogonality condition. Although the orthonormalization process is computationally time-consuming, the results show that it solves the problem of numerical instability for any high order. On the other hand, they are currently conducting new research to improve the computation of discrete moments, such as the group by Sadiq H. Abdulhussain et al. [2], which investigates new methods to take better advantage of the recurrence relationship with respect to the variable x to reduce the numerical instability of classical discrete orthogonal polynomials and computational time.

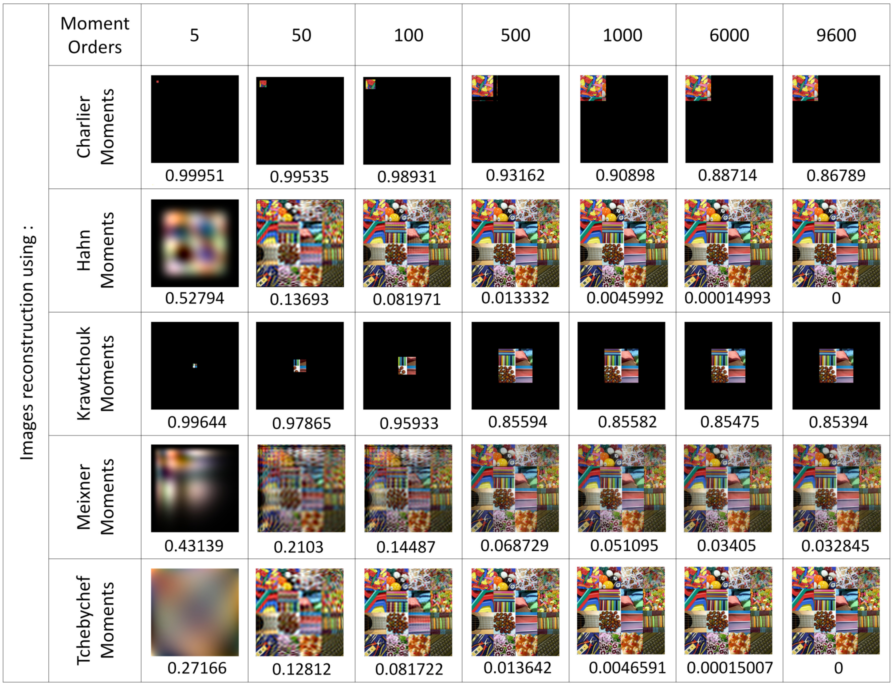

Figure 3.2: Reconstruction and $NIRE_{xy}$ of a FullHD image of size 9600×9600 pixels with different families of classic discrete orthogonal moments.

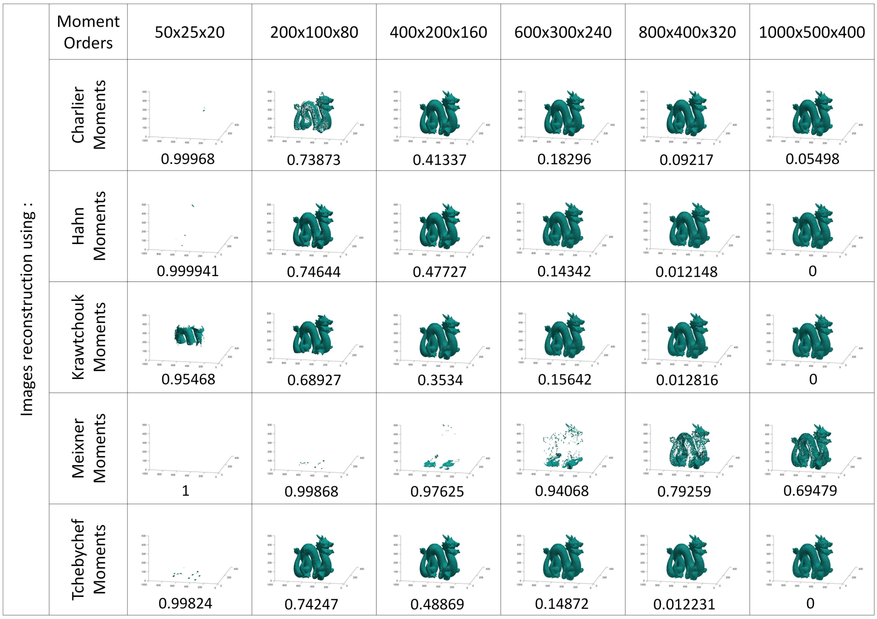

Figure 3.3: Reconstruction and $NIRE_{xyz}$ of the Stanford Dragon of size $400 \times 1000 \times 500$ voxels with different families of classical discrete orthogonal moments.

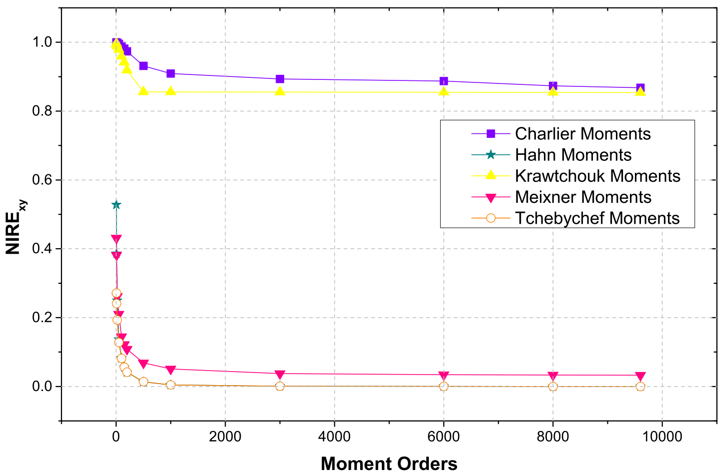

Figure 3.4: $NIRE_{xy}$ of a FullHD image of size 9600×9600 pixels with different families of classic discrete orthogonal moments.

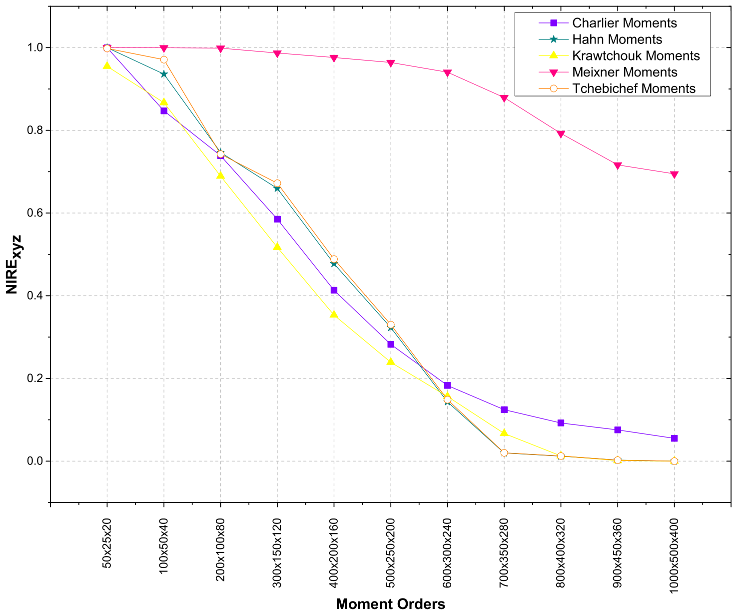

Figure 3.5: $NIRE_{xyz}$ of the Stanford Dragon of size $400 \times 1000 \times 500$ voxels with different families of classical discrete orthogonal moments.

3.5 Conclusions

This chapter analyzes the computation of different families of discrete orthogonal moments for high orders. It also shows the simplification of terms of the recurrence relations with respect to n proposed by Zhu et al. [18]. Also, the Gram-Shmit orthonormalization eliminates the carry error of high-order computation. The results of the reconstruction of images and 3D objects with large dimensions from different types of discrete orthogonal moment families show the effectiveness of the proposed method. Based on the proposal and the analysis presented, it can facilitate the study of various applications that use high resolutions.

References

[1] Alaa M Abdul-Hadi, Sadiq H Abdulhussain, and Basheera M Mahmmod. On the computational aspects of charlier polynomials. *Cogent Engineering*, 7(1):1763553, 2020.

[2] Sadiq H Abdulhussain, Syed Abdul Rahman Al-Haddad, Basheera M Mahmmod, Wissam A Jassim, et al. On computational aspects of tchebichef polynomials for higher polynomial order. *IEEE Access*, 5:2470–2478, 2017.

[3] Nicola Asuni and Andrea Giachetti. Testimages: a large-scale archive for testing visual devices and basic image processing algorithms. In *Eurographics Italian Chapter Conference*, volume 1, page 3, 2014.

[4] César Camacho-Bello and José S Rivera-Lopez. Some computational aspects of tchebichef moments for higher orders. *Pattern Recognition Letters*, 112:332–339, 2018.

[5] Brian Curless and Marc Levoy. A volumetric method for building complex models from range images. In *Proceedings of the 23rd annual conference on Computer graphics and interactive techniques*, pages 303–312, 1996.

[6] Achraf Daoui, Mhamed Sayyouri, and Hassan Qjidaa. Efficient computation of high-order meixner moments for large-size signals and images analysis. *Multimedia Tools and Applications*, pages 1–30, 2020.

[7] Achraf Daoui, Mohamed Yamni, Omar El Ogri, Hicham Karmouni, Mohamed Sayyouri, and Hassan Qjidaa. New algorithm for large-sized 2d and 3d image reconstruction using higher-order hahn moments. *Circuits, Systems, and Signal Processing*, pages 1–26, 2020.

[8] Achraf Daoui, Mohamed Yamni, Hicham Karmouni, Mhamed Sayyouri, Hassan Qjidaa, et al. Stable computation of higher order charlier moments for signal and image reconstruction. *Information Sciences*, 521:251–276, 2020.

[9] Antonio J Durán. Higher order recurrence relation for exceptional charlier, meixner, hermite and laguerre orthogonal polynomials. *Integral Transforms and Special Functions*, 26(5):357–376, 2015.

[10] Basheera M Mahmmod, Alaa M Abdul-Hadi, Sadiq H Abdulhussain, and Aseel Hussien. On computational aspects of krawtchouk polynomials for high orders. *Journal of Imaging*, 6(8):81, 2020.

[11] Ramakrishnan Mukundan. Some computational aspects of discrete orthonormal moments. *IEEE Transactions on Image Processing*, 13(8):1055–1059, 2004.

[12] Ramakrishnan Mukundan, SH Ong, and Poh Aun Lee. Image analysis by tchebichef moments. *IEEE Transactions on image Processing*, 10(9):1357–1364, 2001.

[13] Kenneth H Rosen. *Handbook of discrete and combinatorial mathematics*. CRC press, 1999.

[14] Kar Wai See, Kar-Seng Loke, Poh Aun Lee, and Kia-Fock Loe. Image reconstruction using various discrete orthogonal polynomials in comparison with dct. *Applied Mathematics and Computation*, 193(2):346–359, 2007.

[15] A Venkataramana and P Ananth Raj. Computation of hahn moments for large size images 1. 2010.

[16] P-T Yap, Raveendran Paramesran, and Seng-Huat Ong. Image analysis by krawtchouk moments. *IEEE Transactions on image processing*, 12(11):1367–1377, 2003.

[17] Jian Zhou, Huazhong Shu, Hongqing Zhu, Christine Toumoulin, and Limin Luo. Image analysis by discrete orthogonal hahn moments. In *International Conference Image Analysis and Recognition*, pages 524–531. Springer, 2005.

[18] H Zhu, M Liu, H Shu, H Zhang, and L Luo. General form for obtaining discrete orthogonal moments. *IET image processing*, 4(5):335–352, 2010.

[19] Hongqing Zhu, Min Liu, Yu Li, Huazhong Shu, and Hui Zhang. Image description with nonseparable two-dimensional charlier and meixner moments. *International Journal of Pattern Recognition and Artificial Intelligence*, 25(01):37–55, 2011.